Atypical Quantum Confinement Effect in Silicon Nanowires

Pavel B. Sorokin,*,†,‡,§ Pavel V. Avramov,‡,∥,⊥ Leonid A. Chernozatonskii,§ Dmitri G. Fedorov,# and Sergey G. Ovchinnikov†,‡

Siberian Federal University, 79 Svobodny av., Krasnoyarsk, 660041 Russian Federation, L.V. Kirensky Institute of Physics SB RAS, Krasnoyarsk, 660036 Russian Federation, N. M. Emanuel Institute of Biochemical Physics of RAS, Moscow, 119334 Russian Federation, Fukui Institute for Fundamental Chemistry, Kyoto University, 34-3 Takano Nishihiraki, Sakyo, Kyoto 606-8103 Japan, and Research Institute for Computational Sciences, National Institute of Advanced Industrial Science and Technology (AIST), Central 2, Umezono 1-1-1, Tsukuba, 305-8568 Japan

Received: June 09, 2008; Revised Manuscript Received: July 27, 2008

The quantum confinement effect (QCE) of linear junctions of silicon icosahedral quantum dots (IQD) and pentagonal nanowires (PNW) was studied using DFT and semiempirical AM1 methods. The formation of complex IQD/PNW structures leads to the localization of the HOMO and LUMO on different parts of the system and to a pronounced blue shift of the band gap; the typical QCE with a monotonic decrease of the band gap upon the system size breaks down. A simple one-electron one-dimensional Schrödinger equation model is proposed for the description and explanation of the unconventional quantum confinement behavior of silicon IQD/PNW systems. On the basis of the theoretical models, the experimentally discovered deviations from the typical QCE for nanocrystalline silicon are explained.

Introduction

The field of one-dimensional silicon semiconductor structures is very attractive due to its tremendous technological potential. At present, a number of perfect 1D silicon and silicon−silica nanowires (NW) of various shapes and effective sizes have been synthesized under high temperature conditions.[1−3] The surface of these systems can be saturated by hydrogen or covered by a SiO_2 layer. The TEM images demonstrate the diamond-like crystalline structure of the silicon cores and (in the case of Si/SiO_2 NWs) the amorphous nature of the outer silica layer. All silicon NWs have hemispherical caps terminating one end of the structures. It was shown[4] that the presence of a quantum dot at one end of a nanowire is energetically stable.

The quantum confinement effect (QCE) can be described as the $A + Cd^{-k}$ dependence of the band gap upon the maximum linear size d of nanoparticles, where A, C, and k are sample-dependent parameters. In the following discussion we refer to this monotonous decreasing of the band gap upon the size as *typical*, and any deviation such as an appearance of minima is considered *atypical*. The QCE response of the electronic structure of silicon nanowires has been studied using both experimental and theoretical techniques.[5−8] Typically,[9] the band gap of nanocrystalline silicon depends on the size d as $\sim 1/d$ ($k = 1$).

In some cases considerable deviations from the typical QCE were observed in experiment. For example, Wolkin et al.[10] found that such a deviation occurs for silicon nanocrystallites with a diameter less than 3 nm and attributed it to excitonic effects. Another deviation (a red shift of the band gap accompanying the size decrease) was observed in nanoparticles of strongly correlated electron systems like CuO.[11] A possible reason for the deviations from the typical QCE in silicon nanowires is a quantum dot insertion. The quantum dots divide NWs into nearly independent parts, destroying the typical QCE.

In this work the atypical QCE is analyzed in terms of the localization of the HOMO and LUMO using DFT and semiempirical quantum-chemical calculations as well as by solving a one-electron one-dimensional Schrödinger equation with a step-like potential. It is shown that the quantum dot injection produces potential barriers in the perfect NW structures with a consequent destruction of the typical QCE. The orbital localization shows in a variety of physical properties. For instance, chemical reactivity is connected to it, the intensity of the transitions that determine the efficiency of the nanodevices is related to the transition dipole between the ground and excited states, again affected by the localization; also some electric properties such as conductance may be related to the band gap as well as the localization character.

In contrast to the medium or thick particles, which have square or rectangular cross-sections, the thin (13−70 Å in diameter) nanowires[2,12] have a nearly polygonal or round shapes. Some of them have the [110] main axis with (100) facets.[12] A theoretical model of the atomic structure of pentagonal nanowires (PNW) with the main axis along the [110] direction and five (100) facets was proposed.[13] PNW has a central pentagonal prism as the basis surrounded by several layers of hexagonal prisms and reveals a pronounced segment structure. The pentagonal silicon NWs are the most energetically stable structures[13,14] among several NWs with a small diameter (≤100 Å), designed by connecting triangular prisms cut out along the [110] direction.

The nanowires of pentagonal type with m layers of the hexagonal prisms, surrounding the central pentagonal prism, have (100) facets and n segments and can be compactly classified under the notations of PNW(m,n) where m denotes

* Corresponding author. E-mail: PSorokin@iph.krasn.ru.
† Siberian Federal University.
‡ L.V. Kirensky Institute of Physics SB RAS.
§ N.M. Emanuel Institute of Biochemical Physics of RAS.
∥ E-mail: avramov.pavel@fx2.ecs.kyoto-u.ac.jp.
⊥ Fukui Institute for Fundamental Chemistry, Kyoto University.
Research Institute for Computational Sciences, National Institute of Advanced Industrial Science and Technology (AIST).

10.1021/jp805069b CCC: $40.75
Published on Web 09/11/2008

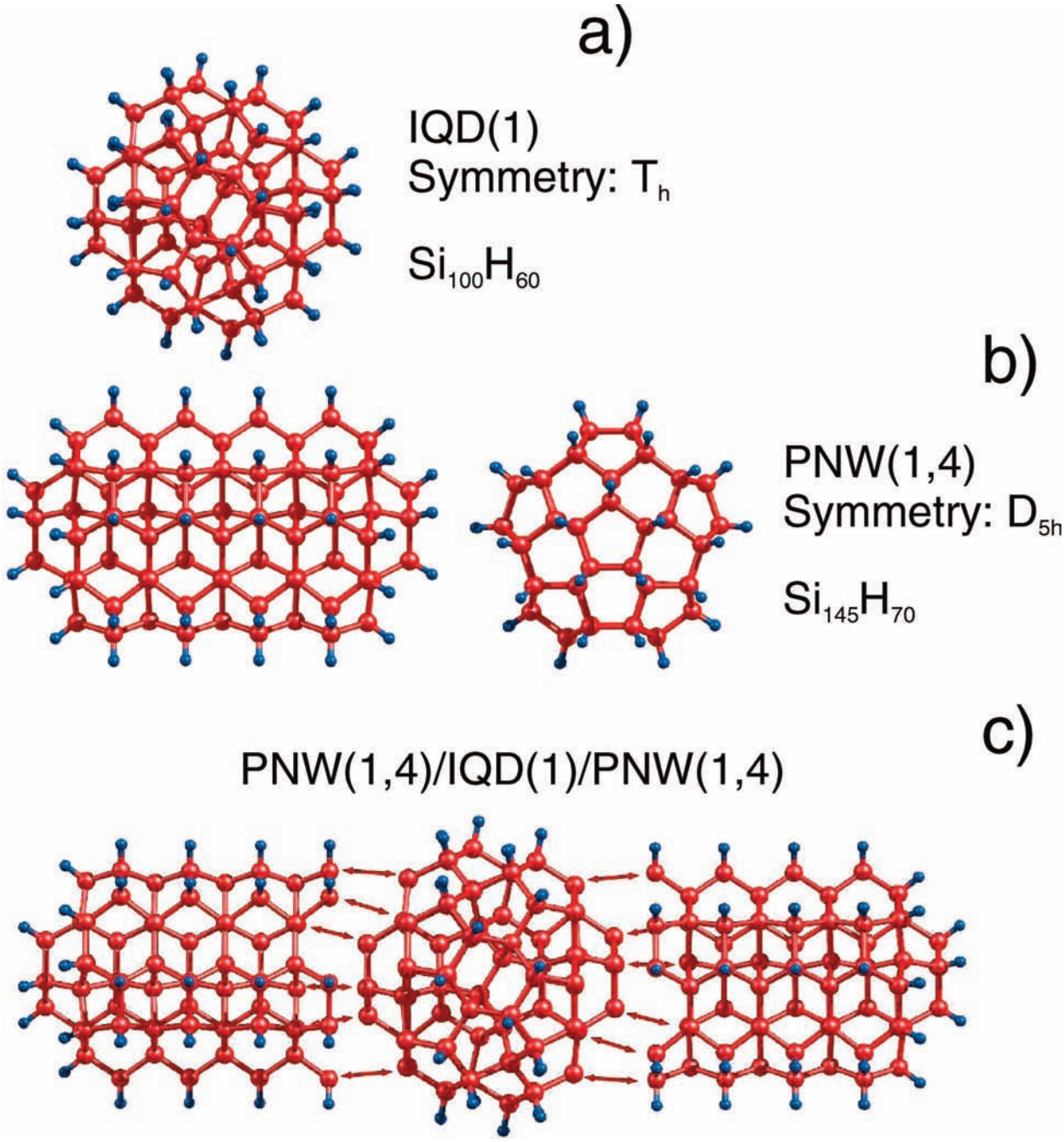

Figure 1. Atomic structure of (a) icosahedral quantum dot IQD(1) ($Si_{100}H_{60}$), (b) pentagonal nanowire PNW(1,4) and (c) the interface in the PNW(1,4)/IQD(1)/PNW(1,4) junction. The silicon atoms of the icosahedral quantum dot core form the pentagon vertexes and IQD/PNW interface. Arrows represent the chemical bonds between IQD and PNW. Silicon and hydrogen atoms are depicted in red and blue, respectively.

the number of hexagonal prism layers along the [110] direction. [13] To explain this better, one can draw analogy to a pencil. The inner pentagonal prism is the pencil graphite core. The addition of hexagonal prisms (larger *m*) make the pencil thicker, and the addition of segments (*n*) make it longer.

Another example of complex silicon nanostructures designed using several crystal units are Goldberg-type quantum dots,[15] including icosahedral quantum dots (IQD)[16,17] as the first member of this family. Depending on the size of parent tetrahedrons, several icosahedral dots with a different number of silicon atoms (Si_{100}, Si_{280}, Si_{600}, Si_{1100}, etc.) can be designed. According to the introduced notation,[4,14] such structures are denoted as IQD(*n*) where *n* is the number of silicon layers surrounding the core. Then the lowest Si_{100} member is denoted as IQD(1) (Figure 1a), whereas the second Si_{280} is denoted as IQD(2). Combining several IQD fragments, one can design a one-dimensional nanowire.[18]

The atomic structure of the IQD(*k*)/PNW(*m*,*n*) interfaces through the pentagonal vertices of the icosahedral dot was propposed in ref 4 (the pentagonal nanowire PNW(1,4) is presented in Figure 1b). The connection of PNW(*m*,*n*) with the pentagonal vertex of the IQD(*k*) can be made through a cavity at the end of PNW(*m*,*n*) formed by five (111) facets obtained by a truncation of the triangular prisms along the [110] directions (see Figure 1c, the bonds between the IQD and PNW are presented as arrows). Such cavity exactly matches both the IQD pentagonal vertex and five (111) facets. The relative stabilities of the objects in this study were not determined directly; the validity of the structures is based on the fact that they are energy minima at the AM1 level of theory.

Methods of Electronic Structure Calculations and Atomic Models

To study the atomic and electronic structure of complex IQD/PNW clusters, we used the semiempirical AM1 method[18] based on the modified neglect of diatomic overlap (MNDO)[19,20] approximation. Previously, the AM1 method was successfully used to study electronic structure of the silicon-based nanoclusters. [15,21] Several dozens or more of possible PNW(1,n_1)/PNW(2,n_2) and IQD(k)/PNW(m,n) junctions can be created. Due to the complexity of the objects ($\sim 10^3$ silicon atoms) and a large number of possible structures, the use of the AM1 semiempirical approach is thought to be reasonable for structure determination and qualitative energetics, although the method systematically overestimates the experimental band gap of silicon nanostructures by about 4.91 eV, as determined from the asymptotic band gap in large nanodots versus the experimental value of crystal silicon.[15] The AM1 band gap overestimation is taken into account in all figures describing the theoretical QCE. To restore the actual AM1 value, one can add 4.91 eV to the band gap values quoted in this work.

The B3LYP/3-21G*[22] method was used to prove the ability of AM1 method to correctly describe the electronic and atomic structure of the objects under study. We calculated the PNW(1,n), IQD(1)/IQD(1) and IQD(1)/PNW(1,n) and found that the results of the electronic structure calculations by both methods are consistent when the AM1 band gap overestimation (4.91 eV) is taken into account. Both methods give close slopes of the QCE dependences, and B3LYP band gaps are 3−4 eV lower than the uncorrected AM1 values.

For example, the B3LYP and AM1 band gaps of the shortest (8 Å) PNW(1,1) are equal to 4.16 and 7.25 eV, respectively (the energy difference is equal to 3.09 eV). The longest PNW(1,4) (20 Å) displays a somewhat larger difference of 3.99 eV (6.80 and 2.81 eV for DFT and AM1, respectively), IQD(1) (13 Å) has a smaller difference of 3.76 eV (7.19 and 3.43 eV for AM1 and DFT, respectively), whereas the formation of the conglomerate IQD(1)/IQD(1) leads to the AM1-B3LYP energy difference of 4.92 eV (6.93 and 2.91 eV for AM1 and DFT, respectively). For the longest IQD(1)/PNW(1,4) system (28 Å), the energy difference between band gaps is equal to 3.97 eV (6.78 and 2.81 eV for AM1 and DFT, respectively).

We also used B3LYP/3-21G* optimized geometries to verify the validity of AM1 for structure prediction. The root-mean-square deviation for PNW(1,4) at the B3LYP/3-21G* and AM1 levels is equal to 0.05 Å. AM1 gives the Si−Si bond lengths a little longer than B3LYP/3-21G*, and both methods predict a high symmetry and similar structures of the silicon nanoclusters.

Results and Discussion

Nanowire Junctions. To study the QCE of the perfect one-dimensional structures, geometries of a set of pristine PNW(1,n) ($n = 1 - 14$) and PNW(2,n) ($n = 1 - 8$) clusters were optimized (Figure 2a) using AM1. The band gaps are shifted relative to each other by 0.15−0.25 eV depending on the length of the objects (Figure 2b). The calculations clearly demonstrate the delocalized character of all valence electrons. The uniform type of delocalization is related to the narrowing of the band gap under the transition from the small clusters to the bulk semiconductors.[23]

The combination of PNW(1,n_1) and PNW(2,n_2) in a joint structure produces the PNW(1,n_1)/PNW(2,n_2) junction with the typical QCE character (Figure 2b). In the short-length region ($\sim$20 Å) the total length of the system is equal to or less than the diameter of PNW(2,n_2) (19.2 Å). Because of this, the band gap of the complex PNW(1,n_1)/PNW(2,n_2) system in this region is close to the band gap of PNW(1,4) with approximately the same length (19.7 Å). For such objects, the localization character of the occupied and vacant levels is such that the orbitals are localized on the PNW(1,n_1) or PNW(2,n_2) arms or delocalized through the whole system. For example, both the HOMO and LUMO of the shortest PNW(1,1)/PNW(2,1) structure are delocalized through the whole system. Elongation of both parts up to 2−5 sections (n_1, $n_2 = 2, 3, 4, 5$) leads to the localization of the HOMO on the PNW(2,n_2) part (Figure 2c). The behavior of the LUMO localization character is such that for the PNW(1,2)/PNW(2,2) structure, the LUMO is mainly localized on the PNW(1,2) part. The consequent elongation of both parts leads to the localization of the LUMO on the PNW(2,n_2) leg (Figure 2c). The intermediate behavior of the QCE for the PNW(1,n_1)/PNW(2,n_2) structure in comparison with the QCE of the pristine PNW(1,n_1) and PNW(2,n_2) nanowires can be explained by the spatial separation of the HOMO and LUMO localized at different parts of the complex nanostructures.

Quantum Dot/Nanowire Junctions. One of the simplest systems with the mirror symmetry is a combination of two IQD(1) and one PNW(m,n) parts in one IQD(1)/PNW(1,n_1)/IQD(1) junction (Figure 3a). The variation of the length of the objects resulting from the addition of PNW(m,n) segments leads to a change of the localization character of the HOMO and LUMO and a consequent change of the QCE (Figure 3b,c). The HOMO and LUMO of the shortest IQD(1)/IQD(1) junction (without PNW(1,n_1) segments between the IQD(1) parts) and IQD(1)/PNW(1,1)/IQD(1) system are delocalized through the whole system. Increasing the number of PNW(1,n_1) segments from 1 to 4 (IQD(1)/PNW(1,2)/IQD(1) system) results in the localization of the HOMO and LUMO at the PNW(1,n_1) part (Figure 3b). A different localization character of the electronic states leads to the appearance of an inflection in the QCE dependence at $L = 25.2-32.9$ Å because of the different slopes of the QCE dependence in the short- and long-range length regions.

Other types of systems with the mirror symmetry are D_{5h} PNW(1,n_1)/IQD(1)/PNW(1,n_1) and PNW(1,n_1)/IQD(2)/PNW(1,n_1) clusters (Figure 4a). We used an equal number of segments in both nanowires. The QCE dependences of both types of structures are presented in Figure 4c. In comparison with PNW(1,n_1), the insertion of the IQD(1) and IQD(2) fragments between the two segments of PNW(1,n_1) produces a blue shift of the band gap at $\sim$0.1 eV. The QCE of PNW(1,n_1)/IQD(1)/PNW(1,n_1) has a larger slope than PNW(1,n_1)/IQD(2)/PNW(1,n_1) because of the different localization character of the HOMO and LUMO. For the small-sized objects ($n_1 = 1, 2$), the HOMO and LUMO are delocalized through the whole system. The absolute values of the band gaps for these cases are determined by the central IQD cores. The IQD(2) has the lowest band gap, so the absolute displacement of the QCE of PNW(1,n_1)/IQD(2)/PNW(1,n_1) systems is determined by the nature of the central core. Increasing the length of PNW(1,n_1) parts in the PNW(1,n_1)/IQD(1)/PNW(1,n_1) systems causes a change in localization character of the HOMO and LUMO: the HOMO is delocalized through the whole system (for $n_1 = 2$)) or localized on the PNW(1,n_1) legs ($n_1 = 3, 4$), whereas the LUMO is localized on the IQD(1) region. Due to the comparatively large size of the of the IQD(2), both the HOMO and LUMO are localized on the central IQD(2) region. Because of the stability of the localization, increasing the total length of the system slightly affects the QCE dependence of the PNW(1,n_1)/IQD(2)/PNW(1,n_1) objects.

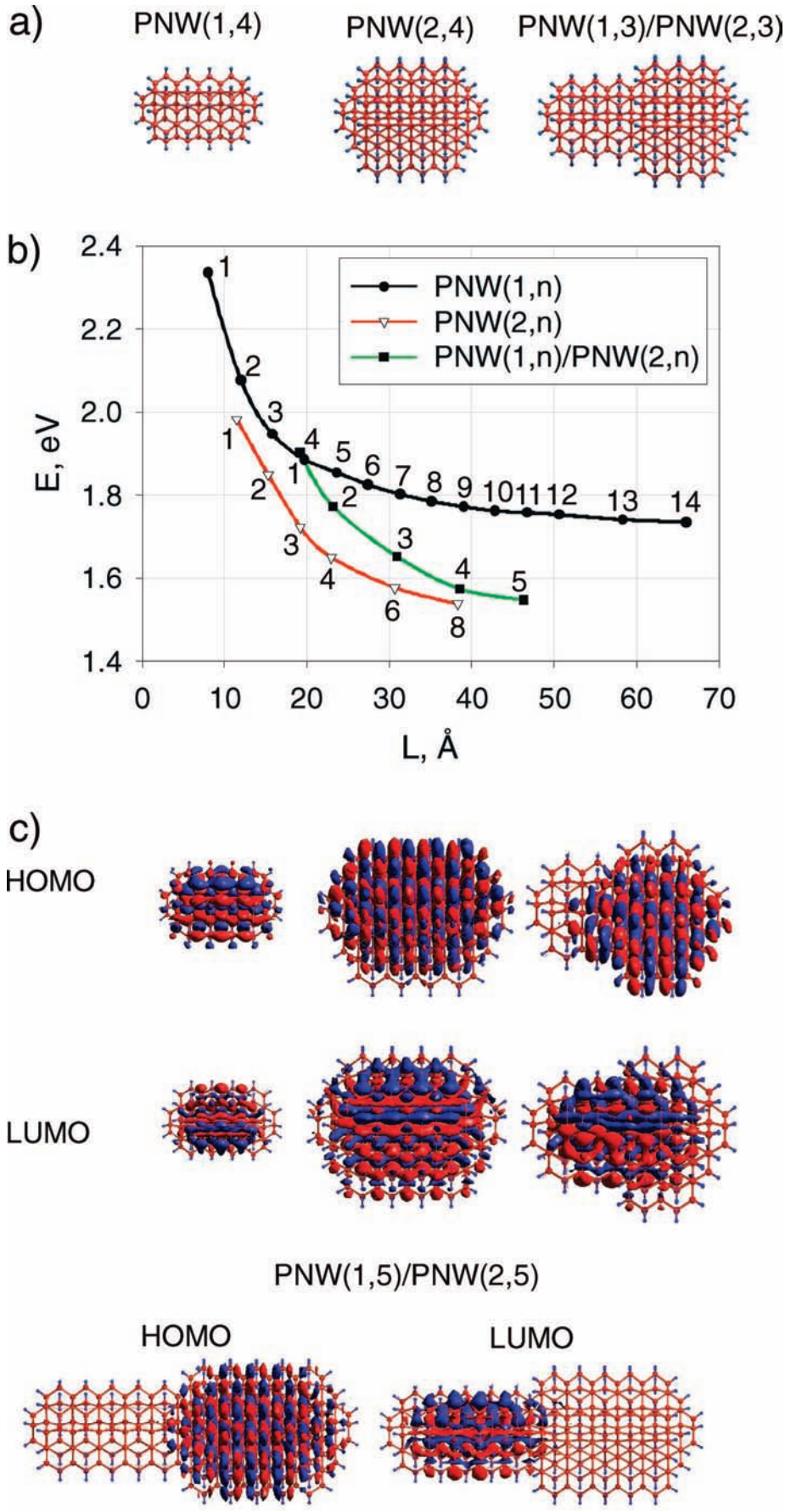

Figure 2. (a) Side view of the pentagonal nanowires (b) dependence of the band gap of PNW(1) (black line with filled circles), PNW(2) (red line with empty triangles) and PNW(1)/PNW(2) (green line with filled squares) upon the total system length (the quantum confinement effect). The values of *n* are shown near the corresponding curve points. The AM1 band gap overestimation (4.91 eV) is taken into account. (c) Spatial localization of the HOMO and LUMO for PNW(1,4), PNW(2,4) and junction PNW(1,2)/PNW(2,2) and PNW(1,5)/PNW(2,5) clusters.

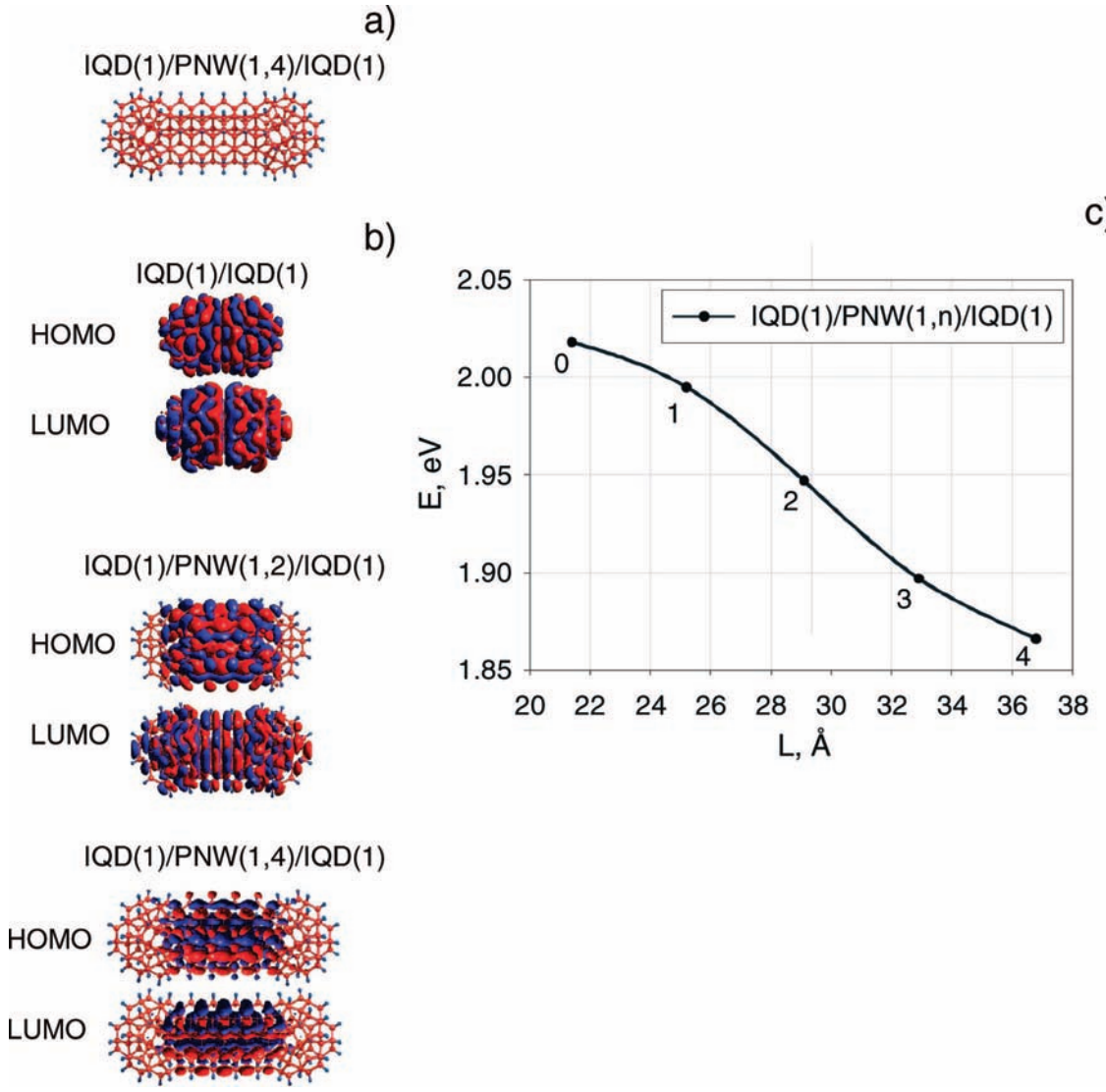

Figure 3. (a) Side view of the IQD(1)/PNW(1,4)/IQD(1) and (b) spatial localization of the HOMO and LUMO for the IQD(1)/IQD(1), IQD(1)/PNW(1,2)/IQD(1) and IQD(1)/PNW(1,4)/IQD(1) clusters. (c) QCE dependence of the band gap of the IQD(1)/PNW(1,*n*)/IQD(1) systems upon the total system length. The values of *n* are shown near the corresponding points of the curve. The AM1 band gap overestimation (4.91 eV) is taken into account.

If the mirror symmetry is broken (asymmetrical IQD(1)/PNW(1,*n*) and PNW(1,*n*)/IQD(1)/PNW(1,*m*) systems, Figure 5a,b), then the typical QCE is completely destroyed (the right side of the curve in Figure 5c, starting at $m > 0$). At the AM1 level of theory the elongation of a single PNW(1,*n*) leg of the IQD(1)/PNW(1,*n*) system up to four segments leads to the typical 1D QCE character (Figure 5c, the left part of the curve for $m = 0$). The HOMO and LUMO (see Figure 5b) of the asymmetrical IQD(1)/PNW(1,*n*) are localized at the PNW(1,*n*) part (HOMO) or delocalized through the whole system including the IQD(1) and the IQD(1)/PNW(1,*n*) interface (LUMO). An appearance of the single PNW(1,1) segment at another side of the system produces a pronounced maximum in QCE (Figure 5c, $n = 4$, $m = 1$) due to the resonance of the orbitals localized on two different PNW parts. The addition of up to six extra segments to one PNW leg keeps the same localization character of the HOMO and LUMO (the longest PNW(1,*n*) leg and IQD(1), respectively, Figure 5b). The second maximum in QCE (symmetrical PNW(1,4)/IQD(1)/PNW(1,4) clusters, $n = 4$, $m = 4$) can be explained by the resonance of the orbitals in both PNW legs.

The quantum dot divides the finite nanowires into almost independent parts. The band gaps of PNW(1,4)/IQD(1)/PNW(1,*n*) ($n = 0, 1, 2, 3, 4$) are nearly equal to the band gap of single PNW(1,4) (1.89 eV, taking into account the AM1 band gap overestimation,[15] Figure 2b). Some discrepancies between the band gaps of clusters and the band gap of PNW(1,4) can be explained by the tunneling effect between the divided nanowire parts via the quantum dot. A further increase in the length of the right part ($n < 4$) leads to the domination of the longest PNW part in the formation of the band gap width and the restoration of the typical QCE behavior (compare the band gaps behavior of PNW(1,4)/IQD(1)/PNW(1,*n*), $n = 4$, 6 and 8 (see Figure 5c) with the band gap behavior of PNW(1,*n*), $n = 4$, 6 and 8 (see Figure 2b). The discrepancies between these curves can be also explained by the tunneling effect.

The complex defect-free nanowire/dot system can be qualitatively described by a simple model based on the solution of one-dimensional Schrödinger equation $(^1/_2\nabla^2 + U(x))\,\psi(x) = \varepsilon\psi(x)$ with the wave function ψ localized in the infinite quantum well[24] and the step potential $U(x)$ shown in Figure 6

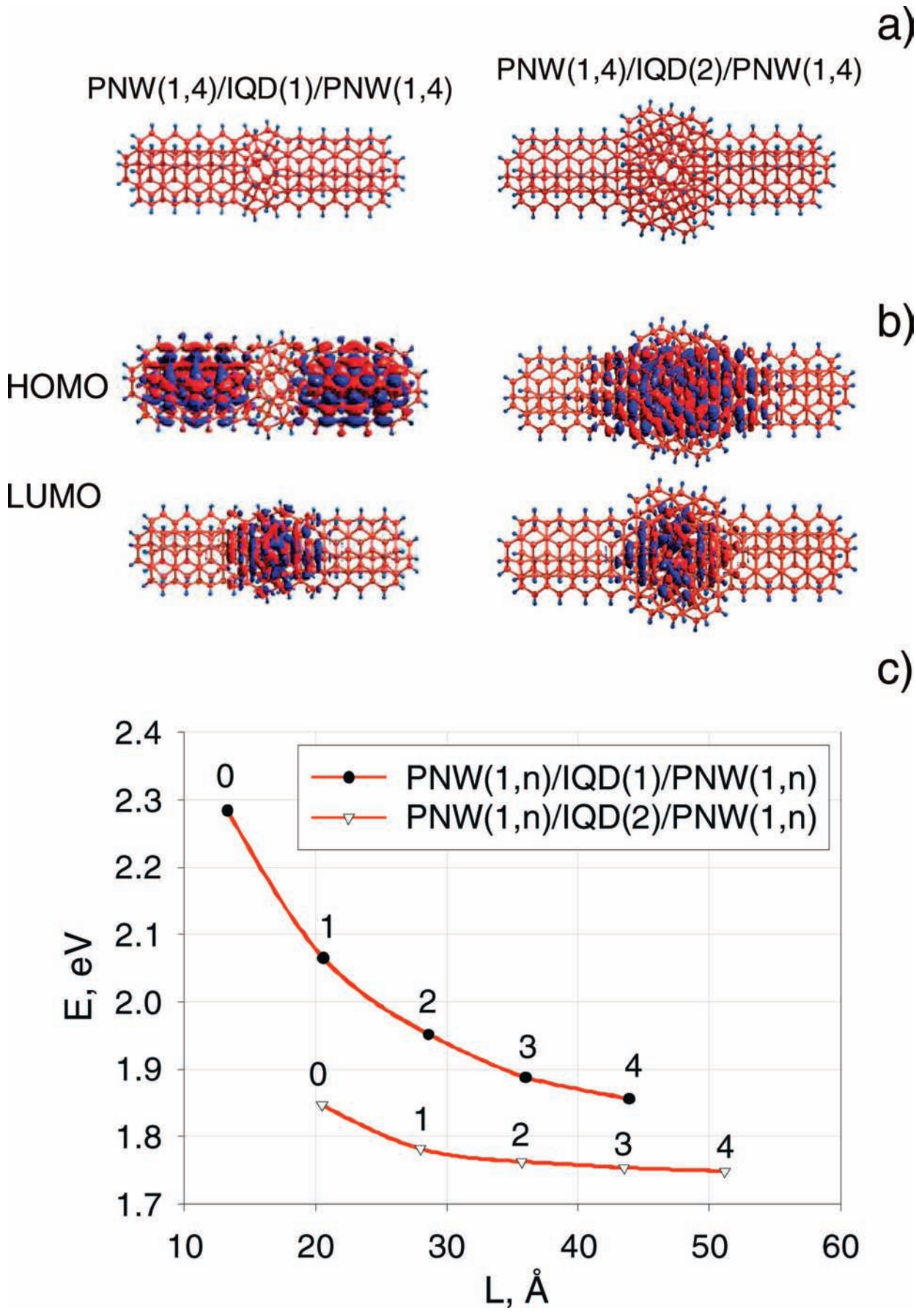

Figure 4. (a) Side view of the PNW(1,4)/IQD(1)/PNW(1,4) and PNW(1,4)/IQD(2)/PNW(1,4) clusters and (b) spatial localization of the HOMO and LUMO for PNW(1,4)/IQD(1)/PNW(1,4) and PNW(1,4)/IQD(2)/PNW(1,4). (c) QCE dependence of PNW(1,*n*)/IQD(1)/PNW(1,*n*) (brown line with solid circles) and PNW(1,*n*)/IQD(2)/PNW(1,*n*) (red line with empty triangles) systems. The values of *n* are shown near the corresponding points of the curves. The AM1 band gap overestimation (4.91 eV) is taken into account.

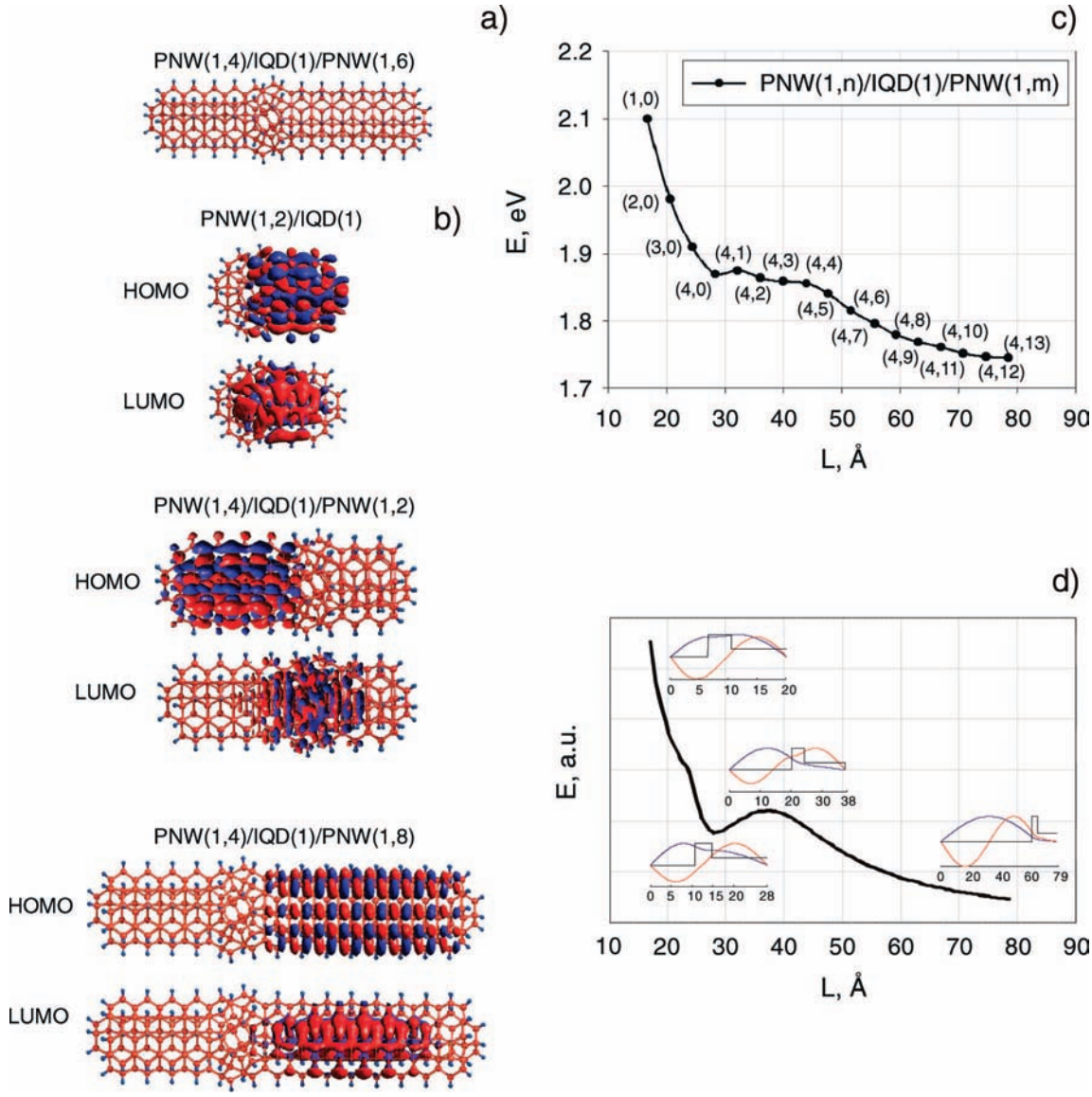

Figure 5. (a) Side view of the PNW(1,4)/IQD(1)/PNW(1,6) cluster. (b) Spatial localization of the HOMO and LUMO for PNW(1,2)/IQD(1), PNW(1,4)/IQD(1)/PNW(1,2) and PNW(1,4)/IQD(1)/PNW(1,8). (c) QCE dependence of PNW(1,*n*)/IQD(1)/PNW(1,*m*) systems, taking into account the AM1 overestimation (4.91 eV). The values of *n* and *m* are shown near the correspondent curve points in pairs as (*n*,*m*). (d) 1D Schrödinger solutions and correspondent QCE. In the insets the spatial distributions of the wave functions of the ground (blue line) and single excited (red line) states are shown.

The IQD(*k*) influence on the electrons near the Fermi level can be taken into account as a quantum barrier with the finite height U_0, whereas the differences between the separate PNW(*l*,*n*) and PNW(*k*,*m*) parts are taken into account by the length of the corresponding wells. For all structures we used the quantum dot barrier height $U = U_0/3$ and a width of 4 Å. The inner nanowire fragment potential was shifted by $U_0 = 0.27$ eV relative to the outer legs.

The quantum confinement of the PNW(1,*n*)/IQD(1)/PNW(1,*m*) system (the dependence of energy difference between the ground and excited levels upon the total system length in atomic units), calculated in this model, is presented in Figure 5d. Like B3LYP and AM1 methods (Figure 5c), the 1D model predicts a decrease of the QCE at the 15−25 Å (the AM1 result is 16.7−28.3 Å) and 39.9−78.0 Å (43.9−78.4 Å) regions. Due to a good qualitative agreement between these results, one can draw the conclusion that the dominant cause of the atypical quantum confinement effect is the change in localization of the HOMO LUMO, related to the ground and excited states.

Some deviations from the AM1 results can be explained by the obvious absence of the interface regions in the proposed model. We believe that the one-electron model can be used for any defect-free elongated systems.

Icosahedral Quantum Dot/Nanowire Mixed Junctions. The complex linear junctions like PNW(1,n_1)/IQD(1)/ PNW(1,*m*)/IQD(1)/PNW(1,n_1) with the mirror symmetry (see Figures 7 and 8) constituting the two IQD(1) and three PNW(1,*k*) parts reveal an atypical QCE dependence with pronounced maxima at 67.7 and 15.3 Å. The first type of the PNW(1,4)/IQD(1)/PNW(1,*m*)/IQD(1)/PNW(1,4) structures is designed by varying the total length of the objects by adding some extra sections to the central PNW(1,*m*) part, keeping the four-sectioned left and right PNW(1,4) cores constant. The longest object has the 83.2 Å length with an eight-section central PNW(1,8).

The atypical QCE of this structure can be explained by a change in localization of the orbitals (see Figure 7b). The HOMO and LUMO are localized at the left and right legs of the system as long as the length of the central part is less or

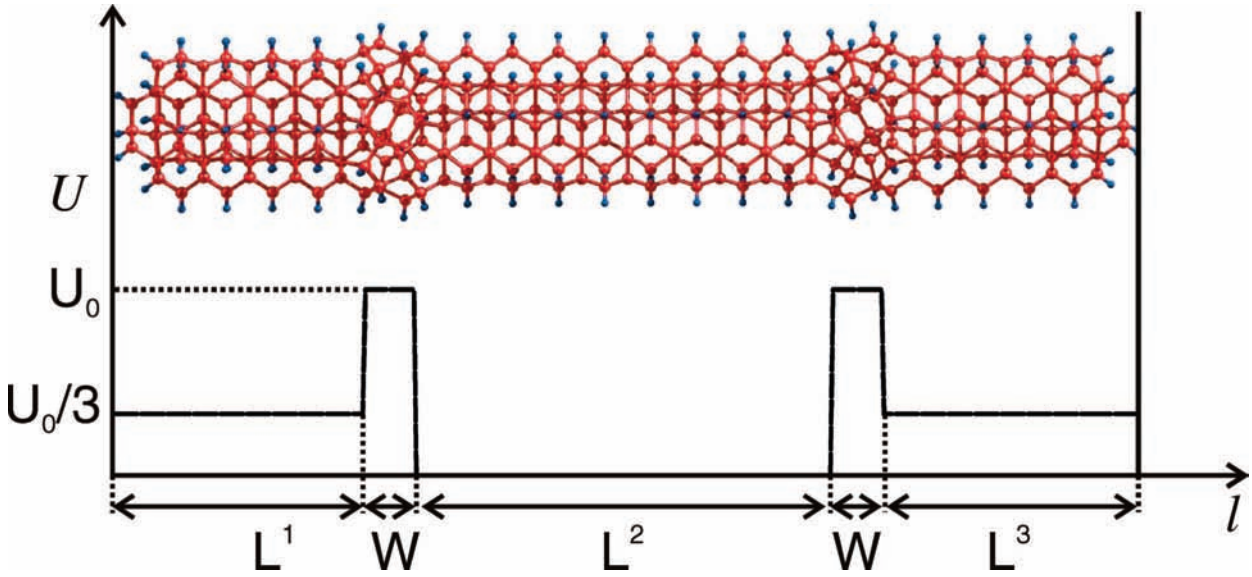

Figure 6. Potential $U(x)$ for the one-dimensional Schrödinger model. The length parameters L^1, L^2 and L^3 are determined by the actual nanowire dimensions. The width W describing the quantum dot width is fixed to 4 Å. U_0 is set to 0.27 eV. The vertical lines at both sides show the infinite walls of the potential.

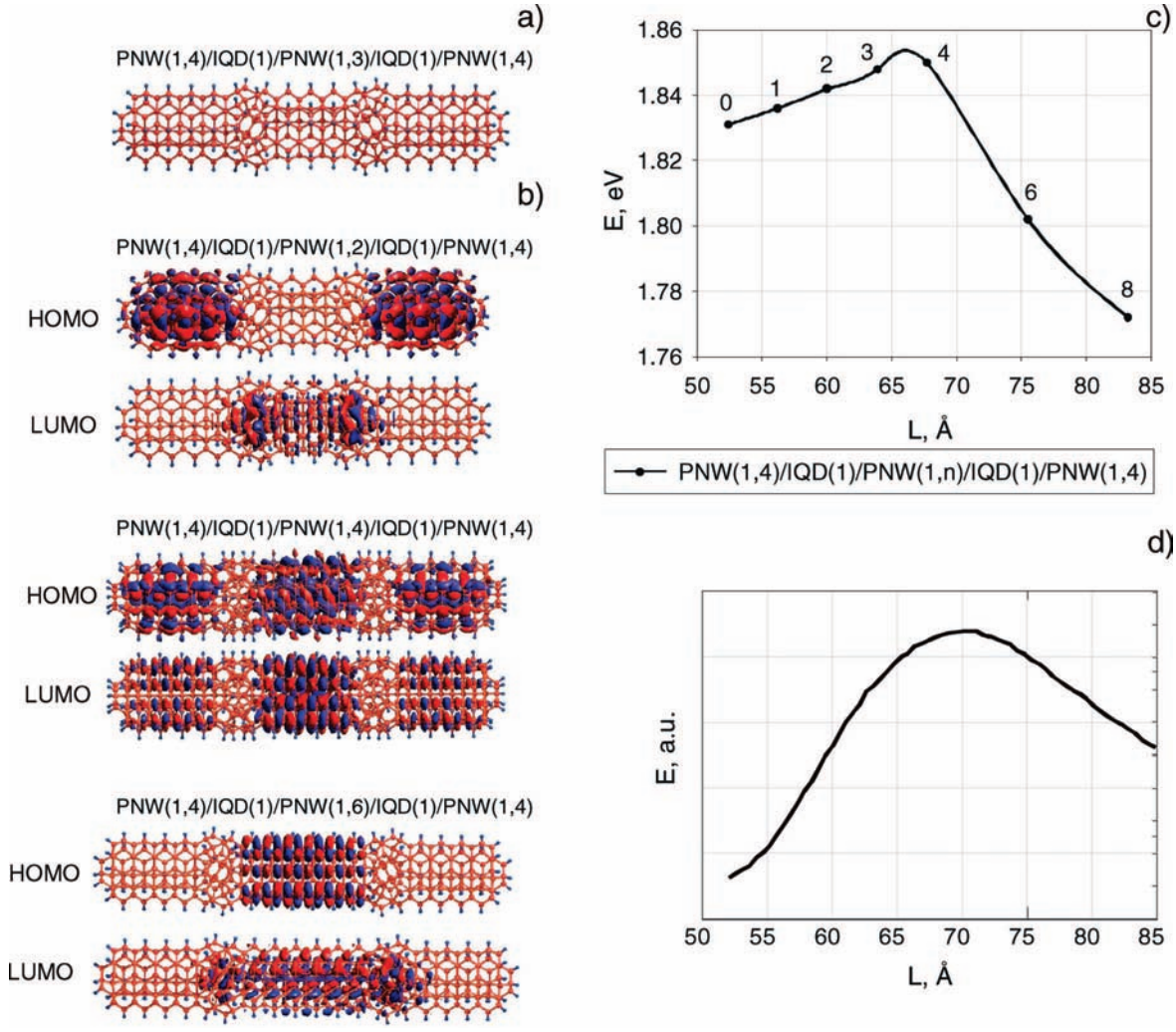

Figure 7. (a) Side view of the PNW(1,4)/IQD(1)/PNW(1,3)/IQD(1)/PNW(1,4) cluster. (b) Spatial localization of the HOMO and LUMO for PNW(1,4)/IQD(1)/PNW(1,2)/IQD(1)/PNW(1,4), PNW(1,4)/IQD(1)/PNW(1,4)/IQD(1)/PNW(1,4) and PNW(1,4)/IQD(1)/PNW(1,6)/IQD(1)/PNW(1,4) clusters. (c) QCE of PNW(1,4)/IQD(1)/PNW(1,*n*)/IQD(1)/PNW(1,4) systems, the AM1 band gap overestimation (4.91 eV) is taken into account. The values of *n* are shown near the correspondent curve points. (d) QCE of the system with two potential barriers calculated using one-dimensional Schrödinger equation.

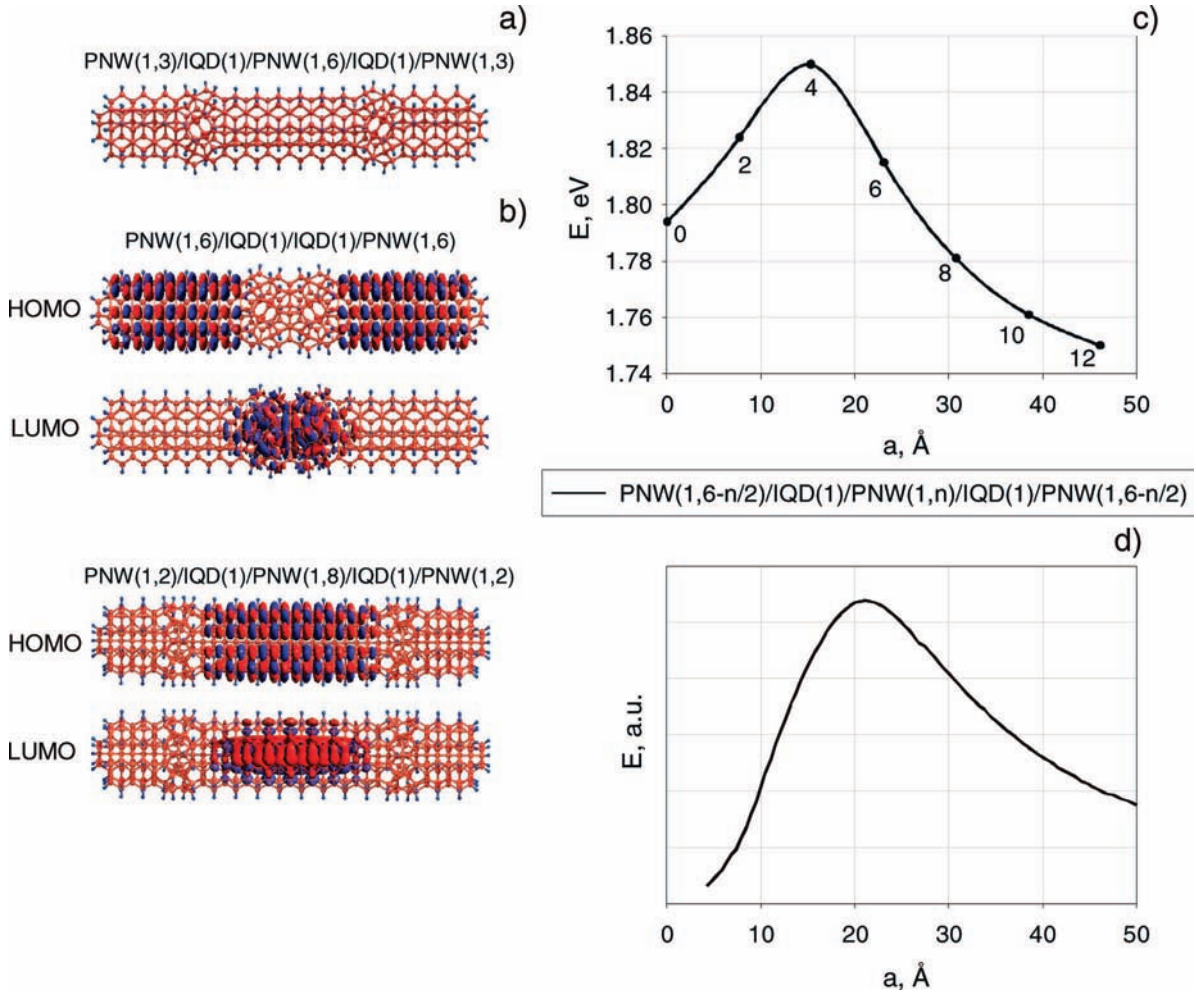

Figure 8. (a) Side view of the PNW(1,3)/IQD(1)/PNW(1,6)/IQD(1)/PNW(1,3) cluster. (b) Spatial localization of the HOMO and LUMO for PNW(1,6)/IQD(1)/IQD(1)/PNW(1,6) and PNW(1,2)/IQD(1)/PNW(1,8)/IQD(1)/PNW(1,2) systems. (c) QCE of PNW(1,6-*n*/2)/IQD(1)/PNW(1,*n*)/IQD(1)/PNW(1,6-*n*/2) systems with the AM1 band gap correction (4.91 eV). The values of *n* are shown near the correspondent curve points. (d) QCE of the system with two potential barriers calculated using the one-dimensional Schrödinger equation.

equal to the length of the two PNW(1,4) legs. The elongation of the central PNW(1,*n*) part ($n \geq 5$) leads to the localization of both the HOMO and LUMO in the central PNW(1,*n*) part.

A small increase of the band gap of PNW(1,4)/IQD(1)/PNW(1,*n*)/IQD(1)/PNW(1,4) ($0 \leq n \leq 4$) can be explained by treating the IQD(1)/IQD(1) system as a composite quantum dot which divides the nanowire into equivalent parts (PNW(1,4) legs). The composite quantum dot has a bigger size than IQD(1) and a smaller band gap. The interaction of the orbitals from the composite quantum dot and PNW legs changes the band gap of the whole system. The consequent increase of the central part ($0 < n \leq 4$) results in a effective transition of the big composite quantum dot into two independent dots with a nanowire between them and higher band gaps.

A further increase of the length of the central part ($n < 4$) leads to the localization of the HOMO on this fragment with consequent decrease of the band gap having a typical QCE behavior (compare band gaps of PNW(1,4)/IQD(1)PNW1,*n*=4,6,8)/IQD(1)/PNW(1,4) (see Figure 7c) with band gaps of PNW(1,*n*=4,6,8) (see Figure 2b). The discrepancies between these curves can be explained by the tunneling effect between the divided nanowire parts via quantum dots.

In Figure 7d the solutions of 1D Schrödinger equation as well as the corresponding QCE are presented. The 1D model potential has two energy barriers. Because of this, the ground and excited levels can be localized on different parts of the system and so the atypical QCE is caused by the complex localization character of one-electron states.

The second type (PNW(1,6-*n*/2)/IQD(1)/PNW(1,*n*)/IQD(1)/PNW(1,6-*n*/2) ($0 \leq n \leq 12$)) of complex linear structures consists of 3 PNW parts and 2 IQD fragments (Figure 8) and keeps the total length of the objects constant (67.6 Å) by simultaneously varying of all PNW(1,*n*) parts. The PNW(1,6)/IQD(1)/IQD(1)/PNW(1,6) system has no central PNW(1) section (the central part is formed by the IQD(1)/IQD(1) fragment) and has two six-sectioned left and right PNW(1,6) legs. On the other side we have the IQD(1)/PNW(1,12)/IQD(1) system with the longest central twelve-sectioned PNW(1,12) part without the left and right PNW(1,*n*) legs. The length of the central PNW(1,12) part is equal to 46.1 Å.

The band gap of the system is determined by the HOMO localized on the left and right legs and the LUMO localized on the IQD(1)/IQD(1) part (Figure 8). The insertion of PNW(1,2) and PNW(1,4) sections between the IQD(1) fragments (and consequent decrease of the left and right legs up to 5 and 4 segments) does not change the nature of the HOMO/LUMO localization. The band gap maximum is observed when the length of the central part (4 segment central PNW part of PNW(1,4)/IQD(1)/PNW(1,4)/IQD(1)/PNW(1,4) system) is 15.3 Å because of the strong interactions of the orbitals of three PNW(1,4) parts, which are similar in length. The consequent increase of the central PNW part (6, 8 and 12 segments) with

the corresponding decrease of the left and right legs results in the restoration of the typical QCE of 1D PNW(1,*n*) system. The solution of one-dimensional Schrödinger equation gives similar result (see Figure 8d).

Conclusions

The quantum confinement effect of the electronic structure of the complex linear junctions of silicon nanowires and quantum dots with different symmetries reveals a pronounced modification or destruction of the typical 1/*d* QCE dependence. The formation of interfaces between constituting parts leads to the localization of the HOMO and LUMO at different parts of nanostructures and a considerable change of the band gaps. The atypical quantum confinement dependence can be also interpreted in terms of the simple one-electron one-dimensional Schrödinger equation based on model step-like potentials. The formation of the 1D complex silicon nanostructures composed of structural units with different symmetries may serve as a promising way to control the band gap. The experimentally observed deviations from typical QCE of silicon nanostructures with the small size[10] can be interpreted as a formation of potential barriers between the *nc*-Si cores with complex localization of the HOMO and LUMO.

Acknowledgment. This work was in part partially supported by a CREST (Core Research for Evolutional Science and Technology) grant in the Area of High Performance Computing for Multiscale and Multiphysics Phenomena from the Japan Science and Technology Agency (JST) as well as by Russian Fund of Basic Researches (grant 08-02-01096) (L.A.C.). P.V.A. acknowledges the encouragement of Dr. Keiji Morokuma, Research Leader at Fukui Institute for Fundamental Chemistry. The geometry of all presented structures was visualized by ChemCraft software.[25] L.A.C. acknowledges I. V. Stankevich for help and fruitful discussions. P.B.S. is grateful to the Joint Supercomputer Center of the Russian Academy of Sciences for access to a cluster computer for quantum-chemical calculations.

References and Notes

(1) Wang, Y.; Schmidt, V.; Senz, S.; Gösele, U. *Nature Natechnol.* **2006**, *1*, 186.
(2) Appel, D. *Nature* **2002**, *419*, 553.
(3) Morales, A. M.; Lieber, C. M. *Science* **1998**, *279*, 208.
(4) Avramov, P. V.; Chernozatonskii, L. A.; Sorokin, P. B.; Gordon, M. S. *Nano Lett.* **2007**, *7*, 20637.
(5) Yeh, C. Y.; Zhang, S. B.; Zunger, A. *Phys. Rev. B.* **1994**, *50*, 14405.
(6) Read, A. J.; Needs, E. J.; Nash, K. J.; Canham, L. T.; Calcott, P. D.; Qteish, A. *Phys. Rev. Lett.* **1992**, *69*, 1232.
(7) Saita, A. M.; Buda, F.; Fiumara, G.; Giaquinta, P. V. *Phys. Rev. B.* **1996**, *53*, 1446.
(8) Pan, H.; Chen, W.; Lim, S. H.; Poh, C. K.; Wu, X.; Feng, Y.; Ji, W.; Lin, J. *J. Nanosci. Nanotechnol.* **2005**, *5*, 733.
(9) Wang, L. L.; Zunger, A. *J. Phys. Chem.* **1994**, *98*, 2158.
(10) Wolkin, M. V.; Jorne, J.; Fauchet, P. M.; Allan, G.; Delerue, C. *Phys. Rev. Lett.* **1999**, *82*, 197.
(11) Ovchinnikov, S. G. *Bull. Russ. Acad. Sci.: Phys.* **2008**, *82*, 156.
(12) Ma, D. D. D.; Lee, C. S.; Au, F. C. K.; Tong, S. Y.; Lee, S. T. *Science* **2003**, *299*, 1874.
(13) Zhao, Y.; Yakobson, B. *Phys. Rev. Lett.* **2003**, *91*, 035501.
(14) Avramov, P. V.; Kuzubov, A. A.; Fedorov, A. S.; Sorokin, P. B.; Tomilin, F. N.; Maeda, Y. *Phys. Rev. B* **2007**, *75*, 205427.
(15) Avramov, P. V.; Fedorov, D. G.; Sorokin, P. B.; Chernozatonskii, L. A.; Gordon, M. S. *J. Phys. Chem. C* **2007**, *111*, 18824.
(16) Zhao, Y.; Kim, Y. H.; Du, M. H.; Zhang, S. B. *Phys. Rev. Lett.* **2004**, *93*, 015502.
(17) Nishio, K.; Morishita, T.; Shinoda, W.; Mikami, M. *J. Chem. Phys.* **2006**, *125*, 074712.
(18) Dewar, M. J. S.; Zoeblish, E. G.; Healy, E. F.; Stewart, J. J. P. *J. Am. Chem. Soc.* **1985**, *107*, 3902.
(19) Stewart, J. J. P. *J. Comput. Chem.* **1989**, *10*, 209.
(20) Sze, S. M. *The Physics of Semiconductor Devices*; Wiley: New York, 1969.
(21) Mazzone, A. M. *Phys. Rev. B* **1996**, *54*, 5970.
(22) (a) Becke, A. D. *Phys. Rev.* **1988**, *A38*, 3098. (b) Lee, C.; Yang, W.; Parr, R. G. *Phys. Rev.* **1988**, *B37*, 785. (c) Barone, V *Chem. Phys. Lett.* **1994**, *226*, 392.
(23) Efros, Al.L.; Efros, A. L. *Sov. Phys. Semicond* **1982**, *16*, 772.
(24) Landau, L. D.; Lifshitz, E. M. Pergamon Press: Oxford, U.K., 1977.
(25) http://www.chemcraftprog.com.

JP805069B